Letters in Applied NanoBioScience
Open-Access Journal (ISSN: 2284-6808)

Article
Volume 14, Issue 2, 2025, 90
https://doi.org/10.33263/LIANBS142.090

Virtual Screening and Identification of Natural Molecules as Promising Quorum Sensing Inhibitors against *Pseudomonas aeruginosa*

Badr-Edine Sadoq [1,*], Yassir Boulaamane [1], Iman Touati [1], Mohammed Reda Britel [1], Amal Maurady [1,2,*]

[1] Laboratory of Innovative Technologies, National School of Applied Sciences of Tangier, Abdelmalek Essaadi University, Tetouan, Morocco
[2] Faculty of Sciences and Techniques of Tangier, Abdelmalek Essaadi University, Tetouan, Morocco
* Correspondence: amal.maurady.ma@gmail.com (A.M.); Sadoq.badredine@etu.uae.ac.ma (B.-E.S.);
Scopus Author ID 36011971000
Received: 8.01.2024; Accepted: 30.06.2024; Published: 15.02.2025

Abstract: In recent years, the increasing spread of antibiotic-resistant bacteria has become one of the most significant public health problems. This resistance is largely due to the formation of biofilms and the expression of virulence factors, which are primarily controlled by a cell communication system called quorum sensing (QS). Therefore, screening a range of compounds for anti-biofilm or anti-QS activities is essential. In *Pseudomonas aeruginosa* (*P. aeruginosa*), a Gram-negative opportunistic human pathogen and one of the leading causes of hospital-acquired infections, QS is regulated by six proteins: LasR, LasI, RhlR, RhlI, PqsR, and PqsA. Stachys species are known for their antimicrobial activity. This study aimed to screen natural molecules from the Stachys database as potential inhibitors of these proteins. A total of 186 molecules from the Stachys database were virtually screened against the selected target proteins. Molecules that qualified were filtered based on Lipinski's rule of five and ADMET properties. Ten potential QS-inhibiting biomolecules were identified: 5-demethylnobiletin, chrysosplenetin, 3'-methoxycalycoptarin, 8-methoxycirsilinol, calycoptarin, casticin, 5-hydroxyauranetin, 5,3',4'-trihydroxy-3,6,7,8-tetramethoxyflavone, syringic acid, and vanillic acid. These molecules were further docked against the six proteins using AutoDockTools to understand the molecular interactions and identify the most effective inhibitor among them. Based on the docking results, chrysosplenetin (ID 5281608) for LasI, 5-demethoxyflavone (ID 358832) for LasR, syringic acid (ID 10742) for RhlR, and 5,3',4'-trihydroxy-3,6,7,8-tetramethoxyflavone (ID 54799) for the proteins RhlI, PqsA, and PqsR were proposed as the best candidates for quorum sensing inhibition in terms of energy and interactions.

Keywords: *P. aeruginosa*; quorum sensing; molecular docking; inhibitors; stachys; Lipinski's rule of five; ADME; virtual screening.

1. Introduction

The growing ability of bacteria that cause disease to resist the antibiotics currently available is a significant challenge for public health [1]. As a result, it is essential to find new ways to fight drug-resistant bacteria, as conventional antimicrobial treatments are becoming less effective. In many types of bacteria that are resistant to multiple drugs, the formation of virulence factors and biofilms is often regulated by a mechanism known as quorum sensing

(QS), which allows bacteria to communicate with each other [2]. This control system allows bacteria to coordinate a collective response to resist the host's immune system and protect themselves from external stressors, including antimicrobial agents [3]. *Pseudomonas aeruginosa* (*P. aeruginosa*) is responsible for 57% of infections acquired in hospitals, particularly in individuals with compromised immune systems due to cystic fibrosis and burn wounds [3,4]. These communication circuits control the expression of a large number of genes that produce virulence factors, such as pyocyanin, proteases, exotoxin A, elastase B, and hydrogen cyanide [2,5,6]. In the Las system, the LasI synthase produces the autoinducer N-(3-oxododecanoyl)-L-homoserine lactone (3-oxo-C12-HSL), which activates the expression of the lasR gene to produce virulence factors like lasB, apr, and toxA.

Additionally, the Las system also positively regulates the Rhl system, which produces the autoinducer N-butanoyl-L-homoserine lactone (C4-HSL) and eventually leads to the production of rhamnolipid and pyocyanin. The third quorum sensing system, known as the Pseudomonas quinolone signal (PQS) system, provides a link between the LasR and RhlR systems and uses signaling molecules like alkyl-4-quinolones (AQs), specifically 2-heptyl-4-hydroxyquinoline (HHQ) and 2-heptyl-3-hydroxy-4(1H)-quinolone (PQS) [7,8]. Due to this, the three quorum sensing systems of *P. aeruginosa* are potential targets for developing new antimicrobial agents.

Most antibiotics are designed to kill bacteria by targeting vital processes necessary for their growth [5]. However, this approach can lead to the development of antibiotic-resistant strains. In contrast, targeting the quorum sensing system, which controls non-essential functions related to a pathogen's virulence, is thought to avoid the problem of resistance [5]. Because of the significant role that quorum sensing plays in microbial pathogenicity, there have been several reported instances of anti-quorum sensing agents in plants and microbes that can weaken the quorum sensing circuit [9].

Plants use a variety of defense strategies to survive in the ecosystem and become a valuable source of antimicrobial agents and other pharmaceutical compounds [10,11]. The genus *Stachys* (*Lamiaceae* family) comprises 300 species widely distributed in tropical and subtropical countries. Different research has confirmed that extracts/constituents of *Stachys* plants have excellent antimicrobial, antioxidant, anxiolytic, anti-inflammatory, cancer-inhibiting, and hypotensive activity [12]. Therefore, plants of the genus Stachys are considered a great source of phytochemical compounds with therapeutic and economic applications [13]. An example of this is a study conducted in 2009 by Dulger and Aki [14], where they looked at the antimicrobial properties of the plant *Stachys pseudopinardii*, which is native to Turkey. They used the MIC and Disc diffusion methods to test the plant's activity against certain pathogens. The results showed that the inhibition zones ranged between 6 and 24 mm. After finishing the micro-dilution test, the lowest concentrations were established as 16 mg/mL for *Stachys pseudopinardii R. Bhattacharjee* and 32 μg/mL for *Hub.–Mor*. (*Lamiaceae*). Phytochemical analysis of the plant revealed the presence of compounds such as diterpenes, phenylethanoid glycosides, flavanoids, and saponines. It is believed that the flavonoids in the plant may be responsible for its antibacterial activity. The study found that *S. pseudopinardii* had significant activity against bacteria and yeast cultures, possibly due to metabolic toxins or the previously mentioned compounds [14].

The present study screened a complete library of natural compounds from the Stachys database to identify potential quorum-sensing inhibitors[15]. The chemical structure of the ligands was obtained in 2D structure coordinates from the Stachys database. These ligands

were then converted into 3D structural coordinates using the Openbabel software. Virtual screening was performed using the PyRX software, and molecules were sorted using various filters, such as the Lipinski rule of five. The sorted molecules were then further analyzed for ADME and toxicity studies. The screened molecules were then docked against the active site of LasI/LasR, RhlI/RhlR, and PqsA/PqsR (Figure 1).

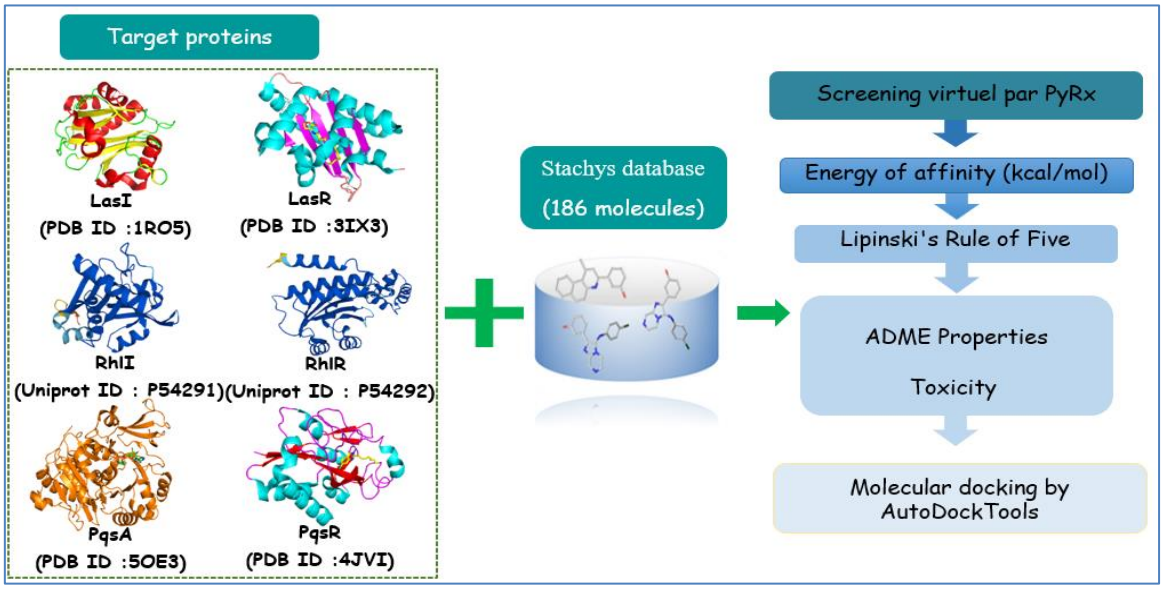

Figure 1. Workflow of the steps followed for virtual screening and sorting of biomolecules from Stachys.

2. Materials and Methods

2.1. Protein preparation.

The crystal structures of the target proteins LasI (PDB ID: 1RO5, resolution = 2.3 Å), LasR (PDB ID: 3IX3, resolution = 1.4 Å), PqsA (PDB ID: 5OE3, resolution = 1.43 Å) and PqsR (PDB ID: 4JVI, resolution = 2.9Å) from *P. aeruginosa* were obtained from the Protein Data Bank with their native ligand (https://www.rcsb.org/). The crystal structures of the target proteins RhII (UniProt ID: P54291) and RhlR (UniProt ID: P54292) were downloaded from the UniProt protein database (https://www.uniprot.org) because they were not available in the Protein Data Bank. Next, the water molecules and native ligands in the crystallographic structure were removed from the protein files, and Kollman charges, Gasteiger charges, and polar hydrogen were added [16].

2.2. Active site prediction.

The prediction of active site residues within these receptors to guide the docking analysis towards these areas was performed using the PrankWeb online tool [https://prankweb.cz/] [17]. The results obtained from the Prankweb active site residue prediction were compared to findings in the literature and confirmed [18–21].

2.3. Ligand library preparation.

The selected ligands as reference for the targets for docking validation and comparison of docking results were downloaded from PubChem in SDF format [https://pubchem.ncbi.nlm.nih.gov/]. They were converted to PDB format using Open Babel [22] and then minimized using Avogadro before being saved in PDBQT format [23]. The tested

natural ligands were downloaded from the Stachys database in PDB format [15]. The database contains about 186 natural compounds.

2.4. Virtual screening.

The virtual screening experiment was performed using PyRx software [24], which is based on AutoDock Vina [25]. This software was used to screen 186 natural compounds from the Stachys database against six selected targets: LasR, LasI, RhlR, RhlI, PqsR, and PqsA. The results of the screening were ranked based on the calculated binding energy. The binding energy of each target's reference ligand was used as a benchmark to establish a threshold score for evaluating the docking results. Only compounds with binding energies lower than the reference ligand were selected, while others were excluded. To further prioritize these molecules, secondary sorting criteria, such as Lipinski's rule of five, ADME properties, and toxicity, were applied [26,27].

2.5. Lipinski's rule of five and ADMET evaluation.

According to this rule, a compound has a good chance of being absorbed orally if it meets at least three of the following four parameters: molecular weight (MW) of less than or equal to 500 (g/mol), calculated LogP of less than or equal to 5, number of hydrogen bond acceptors (HBA) of less than or equal to 10, and number of hydrogen bond donors (HBD) of less than or equal to 5 [28]. For the ADME properties, five parameters were considered to evaluate the pharmacological activity of the selected candidates [29]. These parameters were calculated using the SwissADME server [30]. The analysis of toxicity (hepatotoxicity, carcinogenicity, and mutagenicity) was carried out using the Pro-Tox server [31].

2.6. Molecular docking validation.

Ligands obtained after filtering for ADME and toxicity were further selected for docking against the active site of each protein to gain insight into the binding between inhibitors and proteins. The docking process was carried out using AutoDock 4 software [32].

3. Results and Discussions

3.1. Validation of the accuracy of molecular docking.

The molecular docking protocol was validated by cross-docking co-crystallized ligands with the same parameters used for the studied compounds against different crystal structures (PDB IDs: 3IX3 for LasR, 4JVI for PqsR, and 5OE3 for PqsA). The root-mean-square deviation (RMSD) was calculated through superposition, yielding values below 2 Å, indicating the high quality of the docking program.

3.2. Virtual screening.

A preliminary database screening was conducted using virtual screening with the PyRX software. The reference ligand binding energies were SAM (-7.0 Kcal/mol) for LasI synthase, OHN (-8.0 kcal/mol) for LasR receptor, SAM (-6.5 Kcal/mol) for RhlI synthase, BHL (-6.6 Kcal/mol) for RhlR receptor, 3UK (-9.7 Kcal/mol) for PqsA synthase, and QZN (-7.9 kcal/mol) for PqsR receptor. The screening results led to the selection of 89 molecules for LasI synthase,

64 molecules for LasR receptor, 127 molecules for RhlI synthase, 36 molecules for RhlR receptor, 80 compounds for PqsA synthase, and 73 molecules for PqsR receptor (Figure 2).

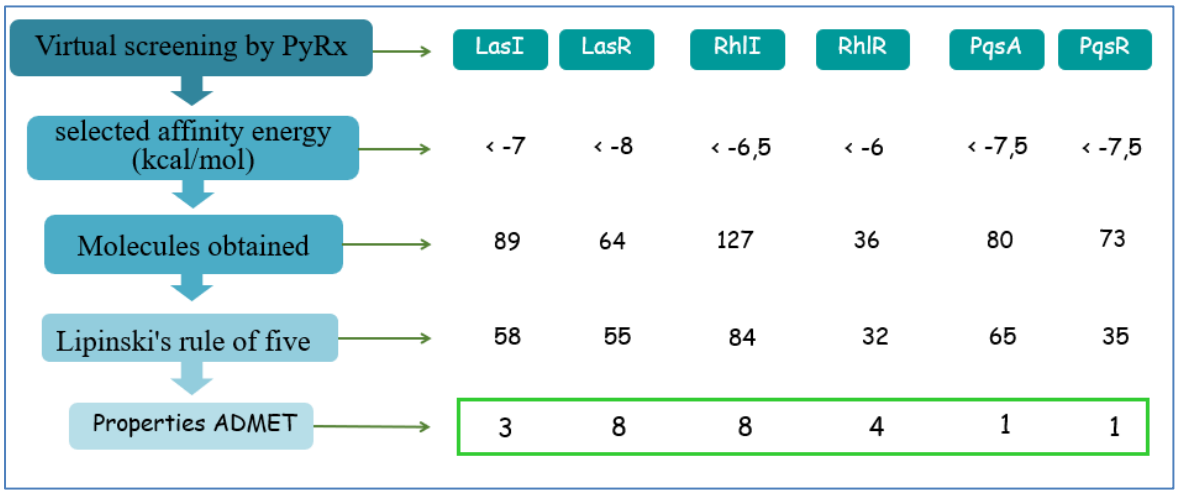

Figure 2. The result of virtual screening, Lipinski, and ADMET filtration of the proteins LasI/LasR, RhlI/RhlR, and PqsA/PqsR.

3.3. ADME and toxicity filters.

The molecules obtained after virtual screening were subjected to Lipinski rule filters, and almost all of them passed the Lipinski filter, meaning they were within the acceptable range. However, 58 molecules for the LasI protein, 55 molecules for LasR, 84 molecules for RhlI, 32 molecules for RhlR, 65 molecules for PqsA, and 35 molecules for PqsR were selected for further study after sorting them based on hydrogen acceptors and hydrogen donors. ADME studies were carried out using SwissADME, which sorted the molecules based on GI absorption, LogKp, P-glycoprotein substrate, BBB permeability, and CYP2D6 inhibitor. 3 molecules for LasI, 8 molecules for LasR, 8 molecules for RhlI, 4 molecules for RhlR, 1 molecule for PqsA, and 1 molecule for PqsR passed the ADME filter and were further selected for toxicity studies using Pro-Tox server (Figure 2).

Ten molecules were selected and found to be safe in toxicity testing. These molecules include 5-Hydroxyauranetin, 8-Methoxycirsilineol, Chrysosplenetin, 3'-Methoxycalycopterin, calycopterin, demethylnobiletin, 5,3',4'-trihydroxy-3,6,7,8-tetramethoxyflavone, casticin, syringic acid, and vanillic acid. The respective properties of these molecules are shown in Table 1.

Table 1. ADME characteristics and toxicity of the final screened compounds.

Molecule	Absorption			Distribution	Metabolism	Toxicity		
	GI absorption	LogKp (cm/s)	P-gp substrate	BBB	CYP2D6 inhibitor	Hepatotoxicity	Carcinogenicity	Mutagenicity
5-Hydroxyauranetin	High	-6.23	No	No	No	Inactive	Inactive	Inactive
8-Methoxycirsilineol	High	-6.52	No	No	No	Inactive	Inactive	Inactive
Chrysosplenetin	High	-6.37	No	No	No	Inactive	Inactive	Inactive

Molecule	Absorption			Distribution	Metabolism	Toxicity		
	GI absorption	LogKp (cm/s)	P-gp substrate	BBB	CYP2D6 inhibitor	Hepatotoxicity	Carcinogenicity	Mutagenicity
3'-Methoxycalycopterin	High	-6.57	No	No	No	Inactive	Inactive	Inactive
Calycopterin	High	-6.37	No	No	No	Inactive	Inactive	Inactive
Demethylnobiletin	High	-6.38	No	No	No	Inactive	Inactive	Inactive
5,3',4'-Trihydroxy-3,6,7,8-tetramethoxyflavone	High	-6.72	No	No	No	Inactive	Inactive	Inactive
Casticin	High	-6.37	No	No	No	Inactive	Inactive	Inactive
Syringic Acid	High	-6.77	No	No	No	Inactive	Inactive	Inactive
Vanillic Acid	High	-6.31	No	No	No	Inactive	Inactive	Inactive

GI absorption: Gastrointestinal absorption; LogKp: Skin permeability value; P-gp: P-glycoprotein; BBB: Blood-brain barrier permeability; CYP2D6 inhibitor: Likeliness of a drug to act as an inhibitor of cytochrome P450 CYP2D6.

These 10 molecules were then docked against the active site of each protein using AutoDock 4 to understand molecular interactions and demonstrate the best possible inhibitor among these molecules.

3.4. Molecular docking.

The results of the interactions between the 10 molecules and the target proteins (LasI, LasR, RhlI, RhlR, PqsA, and PqsR) are reported in Table 2. Additionally, the native ligands SAM (ID34755) of LasI, OHN (ID3246941) of LasR, SAM (ID34755) of RhlI, BHL (ID10130163) of RhlR, 3UK (ID92044056) of PqsA, and QZN (ID71627415) of PqsR were docked against the active site to compare their interactions and binding energies (Table 2). These interactions and binding energies were analyzed using Discovery Studio [33].

Table 2. The binding energies and interacting residues for the final set of screened molecules and the native ligand for the proteins LasI/LasR, RhlI/RhlR, and PqsA/PqsR.

Target proteins	Molecule (PubChem ID)	Binding energy (Kcal/mol)	Hydrogen bonds	Hydrophobic bonds	Pi bonds
LasI	SAM (34755)	-7,33	ARG-30, PHE-105, ILE-107, THR-144, GLU-171	VAL-26, ILE-107	VAL-26(Pi-sigma)
	Chrysosplenetin	-8.43	ARG-30, PHE-105, ILE-107, VAL-143	PHE-27, VAL-26, TRP-33	ARG-30(Pi-cation) PHE-105(Pi-Pi stacking) VAL-26(Pi-sigma) TRP-33(Pi-Pi T-shaped)
	8-Methoxycirsilineol	-7.85	ARG-30, PHE-105, ILE-107, VAL-143	PHE-27, VAL-26, TRP-33	ARG-30(Pi-cation) PHE-105(Pi-Pi stacking) VAL-26(Pi-sigma) TRP-33(Pi-Pi T-shaped)
	5-Hydroxyauranetin	-7.69	ARG-30, ILE-107, THR-144	TRP-33, VAL-143	ARG-30(Pi-cation) VAL-26, PHE-105(Pi-sigma)
LasR	OHN (3246941)	-8.72	TYR-56, TRP-60, ASP-73, SER-129	TYR-64, ALA-70, VAL-76, TRP-88, PHE-101, ALA-105,	-

Target proteins	Molecule (PubChem ID)	Binding energy (Kcal/mol)	Hydrogen bonds	Hydrophobic bonds	Pi bonds
				LEU-110, ALA-127.	
	Demethylnobiletin	-9.6	TRP-60, ARG-61, THR-75, SER-129	LEU-40, ALA-50, VAL-76, CYS-79, PHE-101, ALA-105, LEU-110, ALA-127	TRP-88, LEU-36 (Pi-sigma) Gly-38, TYR-64 (Pi-Pi stacking)
	5-Hydroxyauranetin	-9.56	TRP-60, ARG-61, THR-115, SER-129	LEU-40, ALA-50, VAL-76, PHE-101, ALA-105, LEU-110, ALA-127	LEU-36, TRP-88 (Pi-sigma) ASP-73 (Pi-Anion) TYR-64 (Pi-Pi stacking)
	3'-Methoxycalycopterin	-9.54	TRP-60, ARG-61, THR-115, SER-129, LEU-125	ALA-50, VAL-76, CYS-79, PHE-101, ALA-105, LEU-110, ALA-127	LEU-36, TRP-88 (Pi-sigma) TYR-64 (Pi-Pi stacking)
	Chrysosplenetin	-9.39	TRP-60, ARG-61, THR-115, SER-129, LEU-125	LEU-40, ALA-50, VAL-76, CYS-79 PHE-101, ALA-105, LEU-110, ALA-127	LEU-36, TRP-88 (Pi-sigma) ASP-73 (Pi-Anion) TYR-64 (Pi-Pi stacking)
	Casticin	-9.35	TRP-60, ARG-61, TYR-47, TYR-56	LEU-40, ALA-50, VAL-76, PHE-101, ALA-105, LEU-110, ALA-127	LEU-36, TRP-88 (Pi-sigma) Gly-38, TYR-64(Pi-Pi stacking)
	Calycopterin	-9.19	TYR-56, TRP-60, ARG-61, THR-115, SER-129, LEU-125	ALA-50, VAL-76, CYS-79, PHE-101, ALA-105, LEU-110, ALA-127	LEU-36 (Pi-sigma) TYR-64 (Pi-Pi stacking) ASP-73(Pi-Anion) TRP-88(Pi-sigma)
	8-Methoxycirsilineol	-9.15	TYR-56, ARG-61, THR-115, SER-129, LEU-125	ALA-50, VAL-76, CYS-79, TRP-88 PHE-101, LEU-110, ALA-127	LEU-36, TRP-88 (Pi-sigma) Gly-38, TYR-64 (Pi-Pi stacking) ASP-73(Pi-Anion)
	5,3',4'-Trihydroxy-3,6,7,8-tetramethoxyflavone	-9.0	TYR-56, ARG-61, THR-115, SER-129, LEU-125	ALA-50, VAL-76, CYS-79 PHE-101, LEU-110, ALA-127	LEU-36, TRP-88 (Pi-sigma) Gly-38, TYR-64 (Pi-Pi stacking)
RhlI	SAM (34755)	-6.87	GLY-33, ASP-35, VAL-138, LYS-164	LEU-80, LEU-168	TRP-34 (Pi-anion)
	5,3',4'-Trihydroxy-3,6,7,8-tetramethoxyflavone	-7.33	ASP-35, VAL-138, ARG-104, LYS-164	TRP-34, VAL-138, LYS-164	TRP-34 (Pi-stacking) LEU-80 (Pi-sigma)
	Chrysosplenetin	-7.27	ASP-35, VAL-138, LYS-164	TRP-34, VAL-138, LYS-164, LEU-168	TRP-34 (Pi-stacking) LEU-80 (Pi-sigma)
	3'-Methoxycalycopterin	-7.22	ASP-35, VAL-138, ARG-104, LYS-164	TRP-34, VAL-138, LYS-164	TRP-34 (Pi-stacking) LEU-80 (Pi-sigma)
	Calycopterin	-7.18	ASP-35, VAL-138, LYS-164	TRP-34, VAL-138, LYS-164	TRP-34 (Pi-stacking) LEU-80 (Pi-sigma)
	Demethylnobiletin	-7.15	ASP-35, VAL-138, LYS-164	TRP-34, VAL-138, LYS-164	TRP-34 (Pi-stacking) LEU-80 (Pi-sigma)
	Casticin	-7.13	ASP-35, VAL-138, ARG-104	TRP-34, VAL-138, LYS-164	TRP-34 (Pi-stacking) LEU-80 (Pi-sigma)
	8-Methoxycirsilineol	-7.11	ASP-35, LYS-164	TRP-34, LEU-80, VAL-138, LYS-164, LEU-168	TRP-34 (Pi-stacking)
	5-Hydroxyauranetin	-7.1	ASP-35, LYS-164	TRP-34, LEU-80, VAL-138, LYS-164	TRP-34 (Pi-stacking)
RhlR	BHL (10130163)	-6.46	Trp-68, Asp-81	Ala-44, Val-60, Tyr-72, Ile-84, Phe-101, Leu-107, Ala-111	Trp-96 (Pi-sigma)
	Syringic Acid	-4.66	TRP-68, THR-121	TYR-64, ALA-83 LEU-107, TRP-108 PHE-101, ALA-111	TYR-72(Pi-sigma) ASP-81 (Pi-Anion) TYR-96 (Pi-Pi stacked)
	Vanillic Acid	-4.44	TRP-68, THR-121	ALA-44, ALA-83 ILE-84, VAL-133	TYR-72(Pi-sigma) ASP-81 (Pi-Anion)

Target proteins	Molecule (PubChem ID)	Binding energy (Kcal/mol)	Hydrogen bonds	Hydrophobic bonds	Pi bonds
					TYR-96 (Pi-Pi stacked)
	8-Methoxycirsilineol	-4.12	TRP-68, GLN-73	ASP-81, ALA-83 ILE-84, TRP-96 VAL-133	VAL-60(Pi-sigma) LEU-69(Pi-sigma) TYR-72 (Pi-Pi stacked)
	5,3',4'-Trihydroxy-3,6,7,8-tetramethoxyflavone	-1.23	TRP-68, GLN-73, THR-58, SER-135	LEU-69, ALA-83 ILE-84, VAL-133 TRP-96	VAL-60(Pi-sigma) TYR-72 (Pi-Pi stacked)
PqsA	3UK (92044056)	-9.35	GLY-279, ASP-299, GLY-300, THR-304, ASP382	ALA-278, PRO-281, ILE-301	GLU-305 (Pi-Anion) SER-280, HIS-308 (Pi-Pi stacked)
	5,3',4'-Trihydroxy-3,6,7,8-tetramethoxyflavone	-9.04	GLY-279, ASP-299, THR-323	TYR-211, ALA-278, PRO-281, VAL-309	ILE-301 (Pi-sigma)
PqsR	QZN (71627415)	-7.36	LEU-207	Ala-102, Pro-129, Ile-149, Ala-168, Leu-197, Leu-208, Phe-221, Pro-238	Ile-236 (Pi-sigma)
	5,3',4'-Trihydroxy-3,6,7,8-tetramethoxyflavone	-7.58	LEU-207, ALA-102, THR-265	PRO-210, VAL-211 PRO-238, PHE-221 MET-224	ILE-149 (Pi-sigma), ALA-168(Pi-sigma), LYS-167 (Pi-Pi stacked)

For the LasI protein, the 3 selected molecules underwent re-docking against the protein. A single conformation was chosen for each molecule based on superposition with the reference ligand SAM, which had a binding energy of -7.33 Kcal/mol and formed hydrogen bonds with 5 active site residues of LasI (ARG-30, PHE-105, ILE-107, THR-144, GLU-171). The formed complex (LasI-SAM) was stabilized by 3 hydrophobic interactions (Figure 3). A crystal structure study found that the N-terminal residue of LasI, consisting mainly of Phe27, Arg30, and Trp33, forms the SAM binding pocket, and Phe105 is a conserved residue for the acyl-chain binding tunnel [34]. The selected candidates showed lower affinity energy than the reference ligand, with Chrysosplenetin having the strongest binding affinity of -8.43 Kcal/mol towards LasI. This molecule formed hydrogen bonds with key active site residues, ARG-30, PHE-105, and ILE-107, which are crucial for stabilizing the complex and forming a SAM binding pocket [35]. The interaction of Chrysosplenetin with the AHL synthase of *P. aeruginosa* has a positive effect, suggesting that it may disrupt the synthesis of the autoinducer and impact quorum sensing.

LasR is the activating transcription factor for the virulence genes in *P. aeruginosa* [36]. Molecular docking results showed that the native ligand 3-oxo-C12-HSL had a strong binding energy of -8.72 Kcal/mol. This was due to the formation of four hydrogen bonds between OHN and LasR active sites involving TYR-56, TRP-60, ASP-73, and SER-129 residues (Figure 3). These interactions play a crucial role in the correct folding of LuxR family proteins [37]. The results match those published in the literature [38,39]. Other hydrophobic interactions involving TYR-64, ALA-70, VAL-76, TRP-88, PHE-101, ALA-105, LEU-110, and ALA-127 residues also stabilize the formed complex. Of the 8 selected molecules, Demethylnobiletin showed the best binding energy (-9.6 kcal/mol) towards LasR, formed by hydrogen bonds with TRP-60, ARG-61, THR-75, and SER-129 residues. The attachment of 3-oxo-C12-AHL to LasR triggers the transcription of various virulence genes in P. aeruginosa [40]. The docking

simulations indicated that Demethylnobiletin might interfere with the binding of 3-oxo-C12-AHL to LasR, thus decreasing the expression of QS-controlled genes.

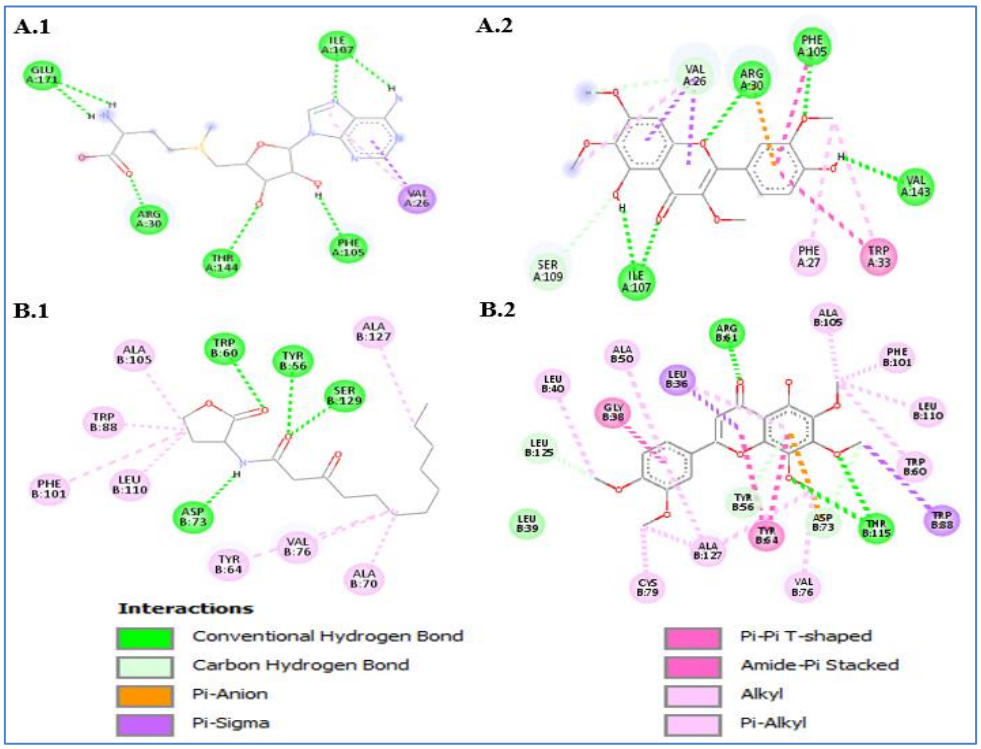

Figure 3. (A.1): 2D representation of the interactions of the ligand SAM with the key residues of the active site of LasI; **(A.2):** 2D representation of the interactions of the potential candidate (Chrysosplenetin) with the active site residues of LasI; **(B.1):** 2D representation of the interactions of the ligand OHN with the key residues of the active site of LasR; **(B.2):** 2D representation of the interactions of the potential candidate (Demethylnobiletin) with the active site residues of LasR.

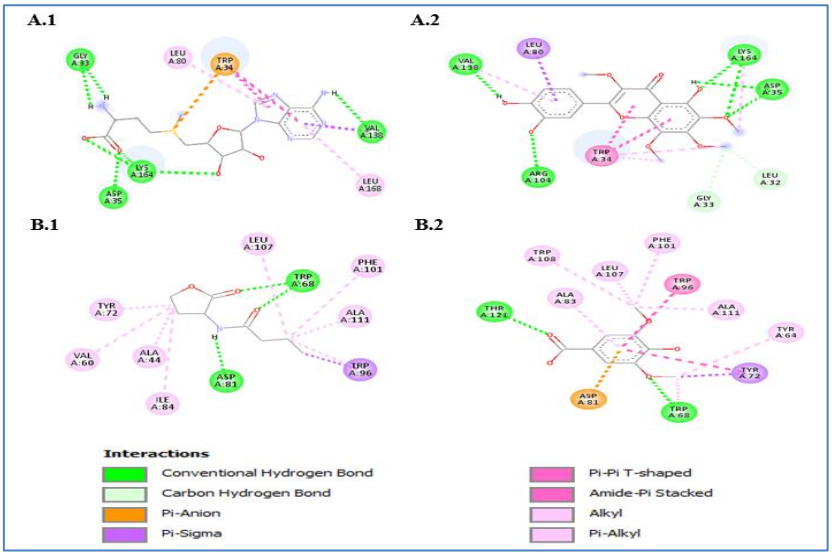

Figure 4. (A.1) 2D representation of the interactions of the ligand SAM with the key residues of the active site of RhlI; **(A.2):** 2D representation of the interactions of the potential candidate (ID 54799-5,3',4'-Trihydroxy-3,6,7,8-tetramethoxyflavone) with the active site residues of RhlI; **(B.1):** 2D representation of the interactions of the ligand BHL with the key residues of the active site of RhlR; **(B.2):** 2D representation of the interactions of the potential candidate (ID 10742- Syringic Acid) with the active site residues of RhlR.

The molecular docking results for protein RhlI showed that the native ligand (SAM) has a low binding energy of -6.87 Kcal/mol and interacts with 4 active site residues (GLY-33, ASP-35, VAL-138, and LYS-164) through hydrogen bonds. SAM also interacts with LEU 80

and LEU 168 through alkyl hydrophobic interactions and with TRP 34 through pi-anion interactions, contributing to the stability of the complex. Of the 8 selected molecules, 5,3',4'-Trihydroxy-3,6,7,8-tetramethoxyflavone had the lowest binding energy (-7.33 Kcal/mol) and formed four hydrogen bonds with ASP-35, VAL-138, ARG-104, and LYS-164. The RhlI-5,3',4'-Trihydroxy-3,6,7,8-tetramethoxyflavone complex was also stabilized by hydrophobic interactions with TRP-34, VAL-138, and LYS-164 and by Pi stacking and Pi sigma interactions with TRP 34 and LEU 80 (Figure 4).

The molecular docking results for protein RhlR showed that the native ligand BHL had a low binding energy of -6.46 Kcal/mol due to two hydrogen bonds with active site residues Trp-68 and Asp-81. The stability of the complex was also due to hydrophobic interactions with residues like Ala-44, Val-60, Tyr-72, Ile-84, Phe-101, Leu-107, and Ala-111 and a pi-sigma bond with residue TRP 96. Our results correlate with the results published in the literature [21]. The four selected molecules had a lower affinity towards RhlR, with binding energies ranging from -4.66 to -1.23 Kcal/mol, compared to BHL. Of these, syringic acid had the lowest binding energy of -4.66 Kcal/mol and formed a complex with RhlR that was stabilized by hydrogen bonds with TRP-68 and THR-121 and hydrophobic interactions (Figure 4).

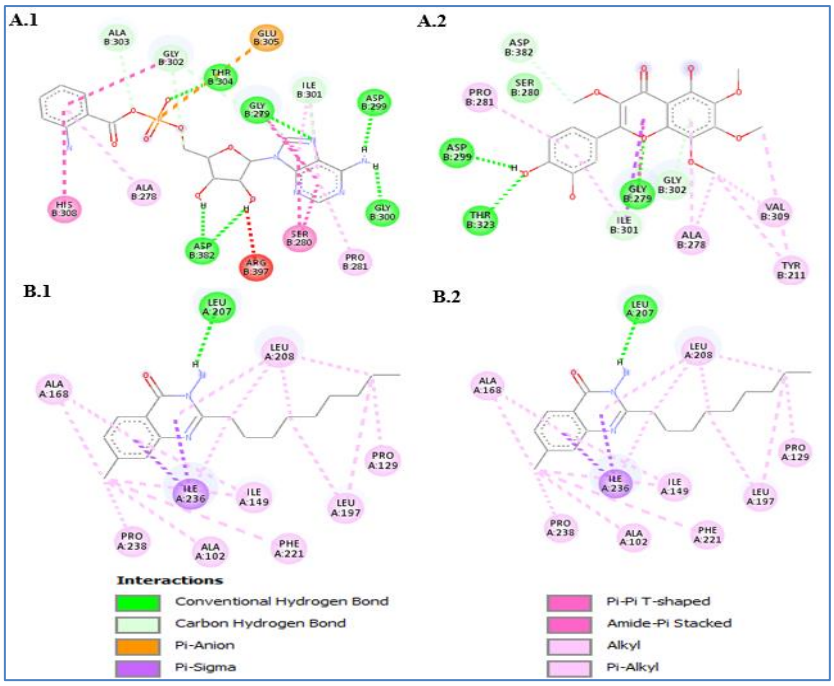

Figure 5. (A.1): 2D representation of the interactions of the ligand 3UK with the key residues of the active site of PqsA; **(A.2):** 2D representation of the interactions of the potential candidate (ID 54799-5,3',4'-Trihydroxy-3,6,7,8-tetramethoxyflavone) with the active site residues of PqsA; **(B.1)** 2D representation of the interactions of the ligand QZN with the key residues of the active site of PqsR; **(B.2):** 2D representation of the interactions of the potential candidate (ID 54799) with the active site residues of PqsR.

The molecular docking results for the PqsA protein showed that the compound 3UK had a strong binding energy of -9.35 Kcal/mol. This strong binding was due to the formation of stable hydrogen bonds with five active site residues of PqsA (Figure 5). The PqsA/3UK complex was also stabilized by alkyl-type hydrophobic interactions with ALA-278, PRO-281, and ILE-3019 residues, as well as pi-anion and pi-stacked interactions with GLU-305, SER-280, and HIS-308 residues. These results are in line with published literature [41]. The molecular docking of molecule ID54799-5,3',4'-Trihydroxy-3,6,7,8-tetramethoxyflavone showed that it had a good interaction energy of -9.04 kcal/mol. This interaction was due to the forming of three hydrogen bonds with the active site residues of PqsA (GLY-279, ASP-299,

and THR-323). This molecule had a similar hydrogen bonding pattern with three amino acids compared to the reference ligand, which interacted with 5 key residues of the PqsA active site (Figure 5).

The molecular docking result of the protein PqsR revealed that the molecule QZN has a binding energy of -7.36 Kcal/mol. This value results from the formation of a single hydrogen bond between QZN and PqsR active site (LEU-207), and the stability of the complex is further enhanced by alkyl-type hydrophobic interactions with residues ALA-102, PRO-129, ILE-149, ALA-168, LEU-197, LEU-208, PHE-221, and PRO-238 and pi-sigma interactions with residue ILE-236. These results are in line with the results published in the literature [42]. Molecule ID54799-5,3',4'-Trihydroxy-3,6,7,8-tetramethoxyflavone, was docked against PqsR and showed better energy of -7.58 Kcal/mol, with hydrogen interactions with residues LEU-207 and ALA-102 and alkyl-type hydrophobic and pi-sigma interactions with residues represented in Figure 5.

The results demonstrated that the molecules from the *Stachys* database could interact with our target proteins. To ensure their bioavailability, molecules with affinity energies lower than those of the reference ligands for each target were subjected to a pharmacological evaluation based on Lipinski's rule of five and ADMET properties. Since the same molecule can show good results for more than one target, we found that a total of 10 molecules distributed as follows: 3 molecules for protein LasI, 8 for LasR, 8 for RhlI, 4 for RhlR, 1 for PqsA, and 1 for PqsR, were found to be in compliance with the rule of five and possess a good pharmacological profile.

The selected molecules underwent re-docking against the proteins to identify the best molecule for each protein. The results showed that Chrysosplenetin was the optimal molecule for LasI, Demethylnobiletin for LasR, 5,3',4'-Trihydroxy-3,6,7,8-tetramethoxyflavone for RhlI, PqsA, and PqsR, and Syringic Acid for RhlR. These molecules exhibited the highest affinity and most favorable interactions compared to the other molecules. These findings highlight the potential of these molecules as promising candidates for further research and development as anti-quorum sensing agents.

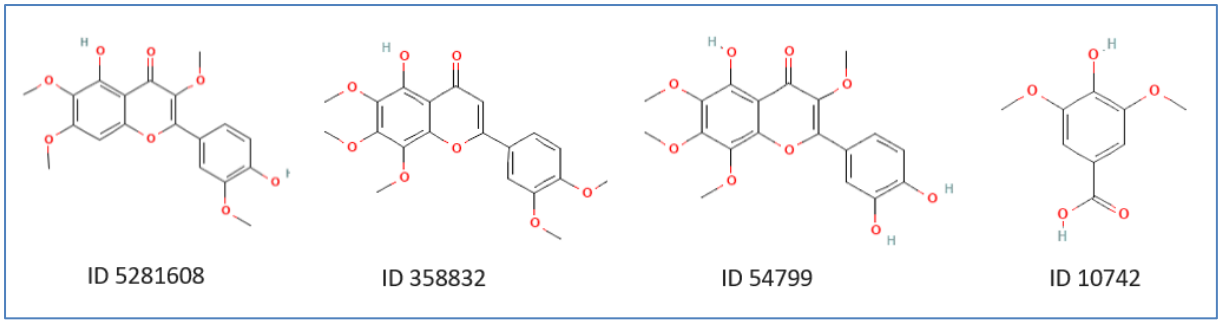

Figure 6. The 2D structures of four selected candidates: (ID 5281608-Chrysosplenetin) for LasI; (ID 358832-Demethylnobiletin) for LasR; (ID 54799-5,3',4'-Trihydroxy-3,6,7,8-tetramethoxyflavone) for RhlI, PqsA, and PqsR; and (ID 10742-Syringic Acid) for RhlR.

Our results indicate that the four molecules belonging to the genus *Stachys* exhibit promising anti-quorum sensing properties. These findings suggest that these molecules have the potential to be considered as candidates for further research and development as anti-quorum sensing agents. Chrysosplenetin (ID 5281608) is a tetramethoxyflavone found in *Stachys. aegyptiaca*, Demethylnobiletin (ID 358832), and 5,3',4'-Trihydroxy-3,6,7,8-tetramethoxyflavone (ID 54799) are both flavonoid compounds found in *Stachys aegyptiaca*,

and Syringic Acid (ID 10742) is a phenolic acid present in *Stachys cretica subsp* [43,44] (Figure 6).

Chrysosplenetin is used to treat breast cancer and anti-enterovirus infections by having antitumor properties and regulating microtubule depolymerization to induce apoptosis of cancer cells [45,46]. Syringic acid, a phenolic compound, displays multiple therapeutic benefits, including antioxidant, anti-inflammatory, anticancer, antidiabetic, antiendotoxic, neuroprotective, cardioprotective, and hepatoprotective properties [47]. Demethylnobiletin exhibits a range of pharmacological effects, including anticancer properties [48], anti-inflammatory effects, antioxidant capabilities, antimicrobial properties, neuroprotective effects, and anti-atherogenic activities [49–53]. Finally, flavonoid 5,3',4'-Trihydroxy-3,6,7,8-tetramethoxyflavone has been shown to possess anti-cancer activity [54].

4. Conclusions

The aim of this study was to discover new inhibitors of quorum sensing that come from natural sources. A collection of natural derivatives from the *Stachys* database was tested against certain proteins (LasI, LasR, RhlI, RhlR, PqsA, and PqsR) found in *P. aeruginosa*. The molecules that were successful were then evaluated for their potential as drugs. Since these molecules originate from natural sources, they have the potential to be both safe and affordable inhibitors of quorum sensing. According to the virtual screening results and considering parameters such as Lipinski's rule, ADME, and toxicity, as well as molecular docking calculation, the molecules Chrysosplenetin (ID 5281608) for LasI, 5-demethoxyflavone (ID 358832) for LasR, Syringic acid (ID 10742) for RhlR, and 5,3',4'-Trihydroxy-3,6,7,8-tetramethoxyflavone (ID 54799) for the proteins RhlI was selected. Further research is needed to confirm these results through *in vitro* and *in vivo* studies.

Funding

Not applicable.

Acknowledgments

We would like to thank the CNRST of Morocco and the Ministry of Higher Education in Morocco for their support of this work.

Conflicts of Interest

The authors declare no conflict of interest.

References

1. Mancuso, G.; De Gaetano, S.; Midiri, A.; Zummo, S.; Biondo, C. The Challenge of Overcoming Antibiotic Resistance in Carbapenem-Resistant Gram-Negative Bacteria: “Attack on Titan.” *Microorganisms* **2023**, *11*, 1912, https://doi.org/10.3390/microorganisms11081912.
2. Zhang, H.; Zhang, Z.; Li, J.; Qin, G. New Strategies for Biocontrol of Bacterial Toxins and Virulence: Focusing on Quorum-Sensing Interference and Biofilm Inhibition. *Toxins* **2023**, *15*, 570, https://doi.org/10.3390/toxins15090570.
3. Wood, S.J.; Kuzel, T.M.; Shafikhani, S.H. Pseudomonas Aeruginosa: Infections, Animal Modeling, and Therapeutics. *Cells* **2023**, *12*, 199, https://doi.org/10.3390/cells12010199.
4. Sathe, N.; Beech, P.; Croft, L.; Suphioglu, C.; Kapat, A.; Athan, E. Pseudomonas Aeruginosa: Infections and Novel Approaches to Treatment “Knowing the Enemy” the Threat of Pseudomonas Aeruginosa and

Exploring Novel Approaches to Treatment. *Infect. Med.* **2023**, *2*, 178–194, https://doi.org/10.1016/j.imj.2023.05.003.

5. Díaz-Pérez, S.P.; Solis, C.S.; López-Bucio, J.S.; Valdez Alarcón, J.J.; Villegas, J.; Reyes-De la Cruz, H.; Campos-Garcia, J. Pathogenesis in Pseudomonas Aeruginosa PAO1 Biofilm-Associated Is Dependent on the Pyoverdine and Pyocyanin Siderophores by Quorum Sensing Modulation. *Microb. Ecol.* **2023**, *86*, 727–741, https://doi.org/10.1007/S00248-022-02095-5.
6. Sadoq, B.-E.; Maalej, R.; Douiri, H.; Britel, M.R.; Bouajaj, A.; Maâlej, R.; Touhami, A.; Abid, M.; Touhami, F.; Maurady, A. A Review on Antibacterial Activity of Nanoparticles. *Biointerface Research in Applied Chemistry* **2022**, *13*, 405, https://doi.org/10.33263/BRIAC135.405.
7. Sadoq, B.E.; Mujwar, S.; Sadoq, M.; Boulaamane, Y.; Britel, M.R.; Bouajaj, A.; Touhami, A.; Touhami, F.; Maurady, A. Metal and Metal Oxide Nanoparticles: Computational Analysis of Their Interactions and Antibacterial Activities Against Pseudomonas Aeruginosa. *Bionanoscience* **2025**, 15, doi:10.1007/s12668-024-01625-4.
8. Vadakkan, K.; Ngangbam, A.K.; Sathishkumar, K.; Rumjit, N.P.; Cheruvathur, M.K. A Review of Chemical Signaling Pathways in the Quorum Sensing Circuit of Pseudomonas Aeruginosa. *Int. J. Biol. Macromol.* **2024**, *254*, 127861, https://doi.org/10.1016/j.ijbiomac.2023.127861.
9. Porzio, E.; Andrenacci, D.; Manco, G. Thermostable Lactonases Inhibit Pseudomonas Aeruginosa Biofilm: Effect In Vitro and in Drosophila Melanogaster Model of Chronic Infection. *Int. J. Mol. Sci.* **2023**, *24*, 17028, https://doi.org/10.3390/ijms242317028.
10. Jeyasri, R.; Muthuramalingam, P.; Karthick, K.; Shin, H.; Choi, S.H.; Ramesh, M. Methyl Jasmonate and Salicylic Acid as Powerful Elicitors for Enhancing the Production of Secondary Metabolites in Medicinal Plants: An Updated Review. *Plant Cell. Tissue Organ Cult.* **2023**, *153*, 447–458, https://doi.org/10.1007/S11240-023-02485-8.
11. Seukep, A.J.; Nembu, N.E.; Mbuntcha, H.G.; Kuete, V. Bacterial Drug Resistance towards Natural Products. *Advances in Botanical Research* **2023**, *106*, 21–45, https://doi.org/10.1016/bs.abr.2022.08.002.
12. Hashemi, S.M.B.; Khodaei, D.; Jahantab, E.; Lacroix, M. Chemical Composition, Antimicrobial, Antioxidant and Cytotoxic Activity of the Essential Oil from the Leaves of Stachys Pilifera Benth. *FEMS Microbiol. Lett.* **2021**, *368*, fnab050, https://doi.org/10.1093/femsle/fnab050.
13. Tomou, E.-M.; Barda, C.; Skaltsa, H. Genus Stachys: A Review of Traditional Uses, Phytochemistry and Bioactivity. *Medicines* **2020**, *7*, 63, https://doi.org/10.3390/MEDICINES7100063.
14. Dulger, G.; Aki, C. Antimicrobial Activity of the Leaves of Endemic Stachys Pseudopinardii in Turkey. *Trop. J. Pharm. Res.* **2009**, *8*, 371–375, https://doi.org/10.4314/tjpr.v8i4.45231.
15. Touati, I.; Abdalla, M.; Ali, N.H.; AlRuwaili, R.; Alruwaili, M.; Britel, M.R.; Maurady, A. Constituents of Stachys Plants as Potential Dual Inhibitors of AChE and NMDAR for the Treatment of Alzheimer's Disease: A Molecular Docking and Dynamic Simulation Study. *J. Biomol. Struct. Dyn.* **2023**, *42*, 1–17, https://doi.org/10.1080/07391102.2023.2217925.
16. Boulaamane, Y.; Khedraoui, M.; Chtita, S.; Touati, I.; Sadoq, B.E.; Britel, M.R.; Maurady, A. Computational Investigation of Phytochemicals from Aloysia Citriodora as Drug Targets for Parkinson's Disease-Associated Proteins. *ChemistrySelect* **2024**, 9, doi:10.1002/slct.202403473.
17. Jendele, L.; Krivak, R.; Skoda, P.; Novotny, M.; Hoksza, D. PrankWeb: A Web Server for Ligand Binding Site Prediction and Visualization. *Nucleic Acids Res.* **2019**, *47*, W345–W349, https://doi.org/10.1093/nar/gkz424.
18. Ilangovan, A.; Fletcher, M.; Rampioni, G.; Pustelny, C.; Rumbaugh, K.; Heeb, S.; Cámara, M.; Truman, A.; Chhabra, S.R.; Emsley, J.; et al. Structural Basis for Native Agonist and Synthetic Inhibitor Recognition by the Pseudomonas Aeruginosa Quorum Sensing Regulator PqsR (MvfR). *PLoS Pathog.* **2013**, *9*, https://doi.org/10.1371/JOURNAL.PPAT.1003508.
19. Majumdar, M.; Dubey, A.; Goswami, R.; Misra, T.K.; Roy, D.N. In Vitro and in Silico Studies on the Structural and Biochemical Insight of Anti-Biofilm Activity of Andrograpanin from Andrographis Paniculata against Pseudomonas Aeruginosa. *World J. Microbiol. Biotechnol.* **2020**, *36*, https://doi.org/10.1007/S11274-020-02919-X.
20. Rex, D.; Saptami, K.; Chandrasekaran, J.; Rekha, P. Pleotropic Potential of Quorum Sensing Mediated N-Acyl Homoserine Lactones (AHLs) at the LasR and RhlR Receptors of Pseudomonas Aeruginosa. *Struct. Chem.* **2023**, *34*, 1327-1339, https://doi.org/10.1007/s11224-022-02115-7.
21. Kumar, L.; Chhibber, S.; Kumar, R.; Kumar, M.; Harjai, K. Zingerone Silences Quorum Sensing and Attenuates Virulence of Pseudomonas Aeruginosa. *Fitoterapia* **2015**, *102*, 84–95,

https://doi.org/10.1016/j.fitote.2015.02.002.
22. O'Boyle, N.M.; Banck, M.; James, C.A.; Morley, C.; Vandermeersch, T.; Hutchison, G.R. Open Babel: An Open Chemical Toolbox. *J. Cheminform.* **2011**, *3*, https://doi.org/10.1186/1758-2946-3-33.
23. Snyder, H.D.; Kucukkal, T.G. Computational Chemistry Activities with Avogadro and ORCA. *J. Chem. Educ.* **2021**, *98*, 1335–1341, https://doi.org/10.1021/ACS.JCHEMED.0C00959.
24. Dallakyan, S.; Olson, A.J. Small-Molecule Library Screening by Docking with PyRx. In Chemical Biology: Methods and Protocols, Hempel, J.E., Williams, C.H., Hong, C.C., Eds.; Springer New York: New York, NY, **2015**; Volume 1263, pp. 243-250, https://doi.org/10.1007/978-1-4939-2269-7_19.
25. Trott, O.; Olson, A.J. AutoDock Vina: Improving the Speed and Accuracy of Docking with a New Scoring Function, Efficient Optimization, and Multithreading. *J. Comput. Chem.* **2010**, *31*, 455-461, https://doi.org/10.1002/JCC.21334.
26. Mandal, M.; Mandal, S. MM/GB(PB)SA Integrated with Molecular Docking and ADMET Approach to Inhibit the Fat-Mass-and-Obesity-Associated Protein Using Bioactive Compounds Derived from Food Plants Used in Traditional Chinese Medicine. *Pharmacological Research - Modern Chinese Medicine* **2024**, 11, doi:10.1016/j.prmcm.2024.100435.
27. Şahin, İ.; Çeşme, M.; Özgeriş, F.B.; Tümer, F. Triazole Based Novel Molecules as Potential Therapeutic Agents: Synthesis, Characterization, Biological Evaluation, in-Silico ADME Profiling and Molecular Docking Studies. *Chem Biol Interact* **2023**, 370, doi:10.1016/j.cbi.2022.110312.
28. Haritha, M.; Sreerag, M.; Suresh, C.H. Quantifying the Hydrogen-Bond Propensity of Drugs and Its Relationship with Lipinski's Rule of Five. *New Journal of Chemistry* **2024**, 48, 4896–4908, doi:10.1039/d3nj05476d.
29. Kalia, M.; Yadav, V.K.; Singh, P.K.; Dohare, S.; Sharma, D.; Narvi, S.S.; Agarwal, V. Designing Quorum Sensing Inhibitors of Pseudomonas Aeruginosa Utilizing FabI: An Enzymic Drug Target from Fatty Acid Synthesis Pathway. *3 Biotech* **2019**, *9*, https://doi.org/10.1007/S13205-019-1567-1.
30. Stegăruș, D.I.; Lengyel, E.; Apostolescu, G.F.; Botoran, O.R.; Tanase, C. Phytochemical Analysis and Biological Activity of Three Stachys Species (Lamiaceae) from Romania. *Plants* **2021**, *10*, 2710, https://doi.org/10.3390/plants10122710.
31. Banerjee, P.; Eckert, A.O.; Schrey, A.K.; Preissner, R. ProTox-II: A Webserver for the Prediction of Toxicity of Chemicals. *Nucleic Acids Res.* **2018**, *46*, W257–W263, https://doi.org/10.1093/nar/gky318.
32. Morris, G.M.; Huey, R.; Olson, A.J. Using AutoDock for Ligand-Receptor Docking. *Curr. Protoc. Bioinforma.* **2008**, *24*, https://doi.org/10.1002/0471250953.bi0814s24.
33. Muthukumar, R.; Karnan, M.; Elangovan, N.; Karunanidhi, M.; Sankarapandian, V.; Venkateswaran, K. Synthesis, Experimental Antimicrobial Activity, Theoretical Vibrational Analysis, Quantum Chemical Modeling and Molecular Docking Studies of (E)-4-(Benzylideneamino)Benzenesulfonamide. *J. Mol. Struct.* **2022**, *1263*, 133187, https://doi.org/10.1016/j.molstruc.2022.133187.
34. Gould, A.; Schweizer, H.P.; Churchill, M.E.A.; Gould, T.A.; Schweizer, H.P.; Churchill, M.E.A. Structure of the Pseudomonas Aeruginosa Acyl-homoserinelactone Synthase LasI. *Wiley Online Libr.* **2004**, *53*, 1135–1146, https://doi.org/10.1111/j.1365-2958.2004.04211.x.
35. McCready, A.R.; Paczkowski, J.E.; Henke, B.R.; Bassler, B.L. Structural Determinants Driving Homoserine Lactone Ligand Selection in the Pseudomonas Aeruginosa LasR Quorum-Sensing Receptor. *Proc. Natl. Acad. Sci. U. S. A.* **2019**, *116*, 245–254, https://doi.org/10.1073/PNAS.1817239116.
36. Kiratisin, P.; Tucker, K.D.; Passador, L. LasR, a Transcriptional Activator of Pseudomonas Aeruginosa Virulence Genes, Functions as a Multimer. *J. Bacteriol.* **2002**, *184*, 4912–4919, https://doi.org/10.1128/JB.184.17.4912-4919.2002.
37. Ahumedo Monterrosa, M.; Galindo, J.F.; Vergara Lorduy, J.; Alí-Torres, J.; Vivas-Reyes, R. The Role of LasR Active Site Amino Acids in the Interaction with the Acyl Homoserine Lactones (AHLs) Analogues: A Computational Study. *J. Mol. Graph. Model.* **2019**, *86*, 113–124, https://doi.org/10.1016/j.jmgm.2018.10.014.
38. Singh, S.; Bhatia, S.; Res, S.P.-J.C.P. In Silico Identification of Polyphenolic Compounds from the Grape Fruit as Quorum Sensing Inhibitors. *Journal of Chemical and Pharmaceutical Research* **2016**, *8*, 411-419.
39. Mohanvel, S.K.; Ravichandran, V.; Kamalanathan, C.; Satish, A.S.; Ramesh, S.; Lee, J.; Rajasekharan, S.K. Molecular Docking and Biological Evaluation of Novel Urea-Tailed Mannich Base against Pseudomonas Aeruginosa. *Microb. Pathog.* **2019**, *130*, 104–111, https://doi.org/10.1016/j.micpath.2019.02.037.
40. Sybiya Vasantha Packiavathy, I.A.; Agilandeswari, P.; Musthafa, K.S.; Karutha Pandian, S.; Veera Ravi,

A. Antibiofilm and Quorum Sensing Inhibitory Potential of Cuminum Cyminum and Its Secondary Metabolite Methyl Eugenol against Gram Negative Bacterial Pathogens. *Food Res. Int.* **2012**, *45*, 85–92, https://doi.org/10.1016/j.foodres.2011.10.022.

41. Dai, L.; Wu, T.; Xiong, Y.; Ni, H.; Ding, Y.; Zhang, W.; Chu, S.; Ju, S.; Yu, J. Ibuprofen-Mediated Potential Inhibition of Biofilm Development and Quorum Sensing in Pseudomonas Aeruginosa. *Life Sci.* **2019**, *237*, 116947, https://doi.org/10.1016/j.lfs.2019.116947.
42. Tomaś, N.; Myszka, K.; Wolko, Ł.; Nuc, K.; Szwengiel, A.; Grygier, A.; Majcher, M. Effect of Black Pepper Essential Oil on Quorum Sensing and Efflux Pump Systems in the Fish-Borne Spoiler Pseudomonas Psychrophila KM02 Identified by RNA-Seq, RT-QPCR and Molecular Docking Analyses. *Food Control* **2021**, *130*, 108284, https://doi.org/10.1016/j.foodcont.2021.108284.
43. El-Ansari, M.A.; Barron, D.; Abdalla, M.F.; Saleh, N.A.M.; Le Quéré, J.L. Flavonoid Constituents of Stachys Aegyptiaca. *Phytochemistry* **1991**, *30*, 1169–1173, https://doi.org/10.1016/S0031-9422(00)95197-5.
44. Bahadori, M.B.; Kirkan, B.; Sarikurkcu, C. Phenolic Ingredients and Therapeutic Potential of Stachys Cretica Subsp. Smyrnaea for the Management of Oxidative Stress, Alzheimer's Disease, Hyperglycemia, and Melasma. *Ind. Crops Prod.* **2019**, *127*, 82–87, https://doi.org/10.1016/j.indcrop.2018.10.066.
45. Sinha, S.; Amin, H.; Nayak, D.; Bhatnagar, M.; Kacker, P.; Chakraborty, S.; Kitchlu, S.; Vishwakarma, R.; Goswami, A.; Ghosal, S. Assessment of Microtubule Depolymerization Property of Flavonoids Isolated from Tanacetum Gracile in Breast Cancer Cells by Biochemical and Molecular Docking Approach. *Chem. Biol. Interact.* **2015**, *239*, 1–11, https://doi.org/10.1016/j.cbi.2015.06.034.
46. Zhu, Q.-C.; Wang, Y.; Liu, Y.-P.; Zhang, R.-Q.; Li, X.; Su, W.-H.; Long, F.; Luo, X.-D.; Peng, T. Inhibition of Enterovirus 71 Replication by Chrysosplenetin and Penduletin. *Eur. J. Pharm. Sci.* **2011**, *44*, 392–398, https://doi.org/10.1016/j.ejps.2011.08.030.
47. Srinivasulu, C.; Ramgopal, M.; Ramanjaneyulu, G.; Anuradha, C.M.; Suresh Kumar, C. Syringic Acid (SA) – A Review of Its Occurrence, Biosynthesis, Pharmacological and Industrial Importance. *Biomed. Pharmacother.* **2018**, *108*, 547–557, https://doi.org/10.1016/j.biopha.2018.09.069.
48. Song, M.; Lan, Y.; Wu, X.; Han, Y.; Wang, M.; Zheng, J.; Li, Z.; Li, F.; Zhou, J.; Xiao, J.; et al. The Chemopreventive Effect of 5-Demethylnobiletin, a Unique Citrus Flavonoid, on Colitis-Driven Colorectal Carcinogenesis in Mice Is Associated with Its Colonic Metabolites. *Food Funct.* **2020**, *11*, 4940–4952, https://doi.org/10.1039/D0FO00616E.
49. Song, M.; Wu, X.; Charoensinphon, N.; Wang, M.; Zheng, J.; Gao, Z.; Xu, F.; Li, Z.; Li, F.; Zhou, J.; et al. Dietary 5-Demethylnobiletin Inhibits Cigarette Carcinogen NNK-Induced Lung Tumorigenesis in Mice. *Food Funct.* **2017**, *8*, 954–963, https://doi.org/10.1039/C6FO01367H.
50. Wang, M.; Meng, D.; Zhang, P.; Wang, X.; Du, G.; Brennan, C.; Li, S.; Ho, C.T.; Zhao, H. Antioxidant Protection of Nobiletin, 5-Demethylnobiletin, Tangeretin, and 5-Demethyltangeretin from Citrus Peel in Saccharomyces Cerevisiae. *J. Agric. Food Chem.* **2018**, *66*, 3155–3160, https://doi.org/10.1021/ACS.JAFC.8B00509.
51. Iwase, Y.; Takemura, Y.; Ju-ichi, M.; Ito, C.; Furukawa, H.; Kawaii, S.; Yano, M.; Mou, X.Y.; Takayasu, J.; Tokuda, H.; et al. Inhibitory Effect of Flavonoids from Citrus Plants on Epstein–Barr Virus Activation and Two-Stage Carcinogenesis of Skin Tumors. *Cancer Lett.* **2000**, *154*, 101–105, https://doi.org/10.1016/S0304-3835(00)00386-4.
52. Trivedi, S.; Maurya, P.; Sammi, S.R.; Gupta, M.M.; Pandey, R. 5-Desmethylnobiletin Augments Synaptic ACh Levels and Nicotinic ACh Receptor Activity: A Potential Candidate for Alleviation of Cholinergic Dysfunction. *Neurosci. Lett.* **2017**, *657*, 84–90, https://doi.org/10.1016/j.neulet.2017.08.010.
53. Yen, J.H.; Weng, C.Y.; Li, S.; Lo, Y.H.; Pan, M.H.; Fu, S.H.; Ho, C.T.; Wu, M.J. Citrus Flavonoid 5-Demethylnobiletin Suppresses Scavenger Receptor Expression in THP-1 Cells and Alters Lipid Homeostasis in HepG2 Liver Cells. *Mol. Nutr. Food Res.* **2011**, *55*, 733–748, https://doi.org/10.1002/MNFR.201000226.
54. Cea, G.F.A.; Etcheberry, K.F.C.; Dulout, F.N. Induction of Micronuclei in Mouse Bone-Marrow Cells by the Flavonoid 5,3′, 4′-Trihydroxy-3,6,7,8-Tetramethoxy-Flavone (THTMF). *Mutat. Res. Lett.* **1983**, *119*, 339–342, https://doi.org/10.1016/0165-7992(83)90182-3.